J Therm Spray Tech (2024) 33:430–446
https://doi.org/10.1007/s11666-023-01701-3

REVIEW

High Entropy Alloy Bond Coats for Thermal Barrier Coatings: A Review

Hossein Shahbazi[1] · Hamideh Vakilifard[1] · Rakesh B. Nair[1] · Andre C. Liberati[1] · Rogerio S. Lima[2] · Pantcho Stoyanov[3] · Christian Moreau[1]

Submitted: 29 June 2023 / in revised form: 9 October 2023 / Accepted: 30 October 2023 / Published online: 26 December 2023

Abstract Thermal barrier coatings (TBCs) are commonly employed as thermal protection systems in harsh environments and are comprised of a ceramic top coat and a metallic bond coat. The traditional materials used for bond coats are MCrAlX alloys, where M represents metals or alloys (such as Ni, Co, or NiCo), and X represents reactive elements like Y, Hf, Ta, and Si. In high-temperature environments, high-entropy alloys (HEAs) have exhibited considerable potential as viable alternatives to bond coat materials, owing to their remarkable mechanical strength, thermal stability, and oxidation resistance. The distinctive compositional characteristics of HEAs can augment bond coat hot corrosion resistance by facilitating the formation of a thermally grown oxide (TGO) characterized by enhanced continuity, density, and uniformity, attributed to the synergistic effects arising from their unique alloying elements. Moreover, HEAs can modulate diffusion phenomena at the interface between the bond coat and substrate, particularly under elevated temperature conditions. This manuscript explores the thermodynamic, mechanical, and microstructural behavior of HEAs, as well as, the selection and application of HEAs as bond coats in comparison to conventional bond coats.

Keywords bond coat · high entropy alloys · mechanical properties · thermal barrier coatings · thermal spray

This article is an invited paper selected from presentations at the 2023 International Thermal Spray Conference, held May 22–25, 2023, in Québec City, Canada, and has been expanded from the original presentation. The issue was organized by Giovanni Bolelli, University of Modena and Reggio Emilia (Lead Editor); Emine Bakan, Forschungszentrum Jülich GmbH; Partha Pratim Bandyopadhyay, Indian Institute of Technology, Karaghpur; Šárka Houdková, University of West Bohemia; Yuji Ichikawa, Tohoku University; Heli Koivuluoto, Tampere University; Yuk-Chiu Lau, General Electric Power (Retired); Hua Li, Ningbo Institute of Materials Technology and Engineering, CAS; Dheepa Srinivasan, Pratt & Whitney; and Filofteia-Laura Toma, Fraunhofer Institute for Material and Beam Technology.

✉ Hossein Shahbazi
hossein.shahbazi@concordia.ca;
hossein.shahbazi@mail.concordia.ca

✉ Christian Moreau
Christian.moreau@concordia.ca

[1] Department of Mechanical, Industrial and Aerospace Engineering, Concordia University, Montreal, QC H3G 1M8, Canada

[2] National Research Council of Canada, 75 de Mortagne Blvd, Boucherville, QC J4B 6Y4, Canada

[3] Department of Chemical and Materials Engineering, Concordia University, Montreal, QC H3G 1M8, Canada

Introduction

Thermal barrier coatings (TBCs) conventionally consist of a ceramic top coat and a metallic bond coat, serving as a vital protective layer for turbine components to mitigate the detrimental effects of severe thermo-mechanical conditions and operating environments (Ref 1). The ceramic top coat, predominantly composed of yttria-stabilized zirconia (YSZ), serves the dual purpose of safeguarding against degradation at elevated temperatures and shielding the underlying layers from thermal cycling-induced stresses experienced by engine components (Ref 2, 3). In contrast, the primary role of the metallic bond coat is to provide protection to the superalloy substrate components against extensive oxidation and corrosion, while simultaneously enhancing the adhesive strength between the ceramic top layer and the substrate components (Ref 4). The most

commonly used materials for bond coats are MCrAlYs (M = Ni, Co, or Ni + Co), since they exhibit excellent mechanical properties and are highly resistant to oxidation and corrosion (Ref 5). In addition, MCrAlYs exhibit lower ductile-to-brittle transition temperature (DBTT) in conjunction with higher chromium content, which enables them to inhibit cracking during thermal cycling (Ref 6). The incorporation of yttrium within MCrAlY coatings effectively impedes the outward diffusion of aluminum, consequently leading to an enhancement in the adhesion of the thermally grown oxide (TGO) scale (Ref 7). The oxide scale of MCrAlY in TBCs, primarily composed of aluminum oxide (Al_2O_3), is an integral part of the functioning mechanism of bond coat systems as it provides insulation, prevents oxidation, and contributes to the overall TBC durability before it reaches a critical thickness (Ref 8). While MCrAlY is well established as a TBC bond coat material, its performance and efficiency at elevated temperatures (>1100 °C) are deteriorated (Ref 9, 10). Since the efficiency of gas turbine engines is directly correlated to their operating temperature, turbine industries are focusing on new TBC systems that would allow them to operate at higher temperatures, thus being more fuel-efficient and sustainable (Ref 9). Due to their stable microstructure and promising mechanical properties at elevated temperatures, high entropy alloys (HEAs) are an emerging class of advanced materials that can be a quality choice for TBC bond coats and replace traditional MCrAlY bond coat systems (Ref 3). HEAs are characterized by equimolar or close to equimolar concentrations of five or more principal elements, with each of the constituent elements ranging between 5 and 35 at.%. Since they have inherently high configurational entropy (>1.5 R, where R is the gas constant), the solid-solution phases of HEAs are stabilized, resulting in oxidation resistance at elevated temperatures (Ref 11). Additionally, other core effects such as lattice distortion, sluggish diffusion, and the cocktail effect contribute to bond coat's enhanced properties, including improved bonding and mechanical strength, fracture toughness, corrosion, oxidation, and creep resistance at high temperatures (Ref 12). Since the demand for HEAs is increasing, the potential benefits of HEAs coupled with thermal spraying technologies can help address numerous challenges associated with TBC systems (Ref 13). Although thermally sprayed HEAs have been studied for several applications, the exploration of thermal sprayed HEAs as TBC bond coats has not been fully explored (Ref 14). Furthermore, although high-velocity oxy-fuel (HVOF) is acknowledged for its capability to generate high-quality bond coats, alternative lower-temperature techniques such as high-velocity air-fuel (HVAF) and cold spraying (CS) present viable means for fabricating HEA coatings. In this way, the powders would not undergo the melting process, hence, reducing in-flight oxidation and improving bond coat properties (Ref 15). The application of CS, HVOF, and HVAF techniques for depositing HEA coatings has attracted attention in bond coat applications, thereby potentially introducing a novel research avenue for TBCs (Ref 14, 16, 17). Therefore, the primary objective of this review is to undertake a comprehensive evaluation and analysis of the material selection process for HEA bond coats, the microstructure characteristics of thermally sprayed HEA bond coats, and the physical properties exhibited by thermally sprayed HEA coatings. A brief explanation of oxidation resistance, coefficient of thermal expansion (CTE), and TGO is presented in this paper, as well as a comparison to conventional bond coats in TBC systems.

Historical Composition of Bond Coats and Selecting HEA Elements for Bond Coat Applications

Historical Bond Coat Composition

Figure 1 briefly summarizes significant milestones in the development of bond coats. Since the 1950 s, diffusion aluminum alloys have been used to protect the hot regions of gas turbine engines due to their low cost and wide availability (Ref 18). During the initial years of the 1970 s, the introduction of NiCrAlY overlay coatings marked a significant advancement in mitigating corrosion and oxidation within the high-temperature regions of industrial equipment, with particular emphasis on gas turbine blades (Ref 19). The predominant challenges faced by coated components subjected to elevated temperatures in oxidizing environments were the occurrence of oxide scale spallation and cracking. In the mid-1970 s, additional investigations were conducted to enhance the stability and adhesion of the Al_2O_3 oxide scale formed on coatings subjected to elevated temperatures. This was achieved by alloying the Al_2O_3 oxide scale with Yttrium (Y), Hafnium (Hf), Platinum (Pt), and Silicon (Si) (Ref 20). During the 1980 s, researchers dedicated their efforts to examining the mechanical properties and compatibility of NiCrAlY coatings when applied to superalloy substrates. Within this timeframe, scientific investigations focused on enhancing the mechanical characteristics of NiCrAlY coatings and establishing compatibility between the coating layer and the superalloy substrate. These objectives were successfully accomplished through the addition of tantalum (Ta) as an alloying element to the NiCrAlY coatings. A variety of NiCrAlY coatings with different chromium (Cr) and aluminum (Al) contents have been developed to meet the diverse environmental and technological conditions found

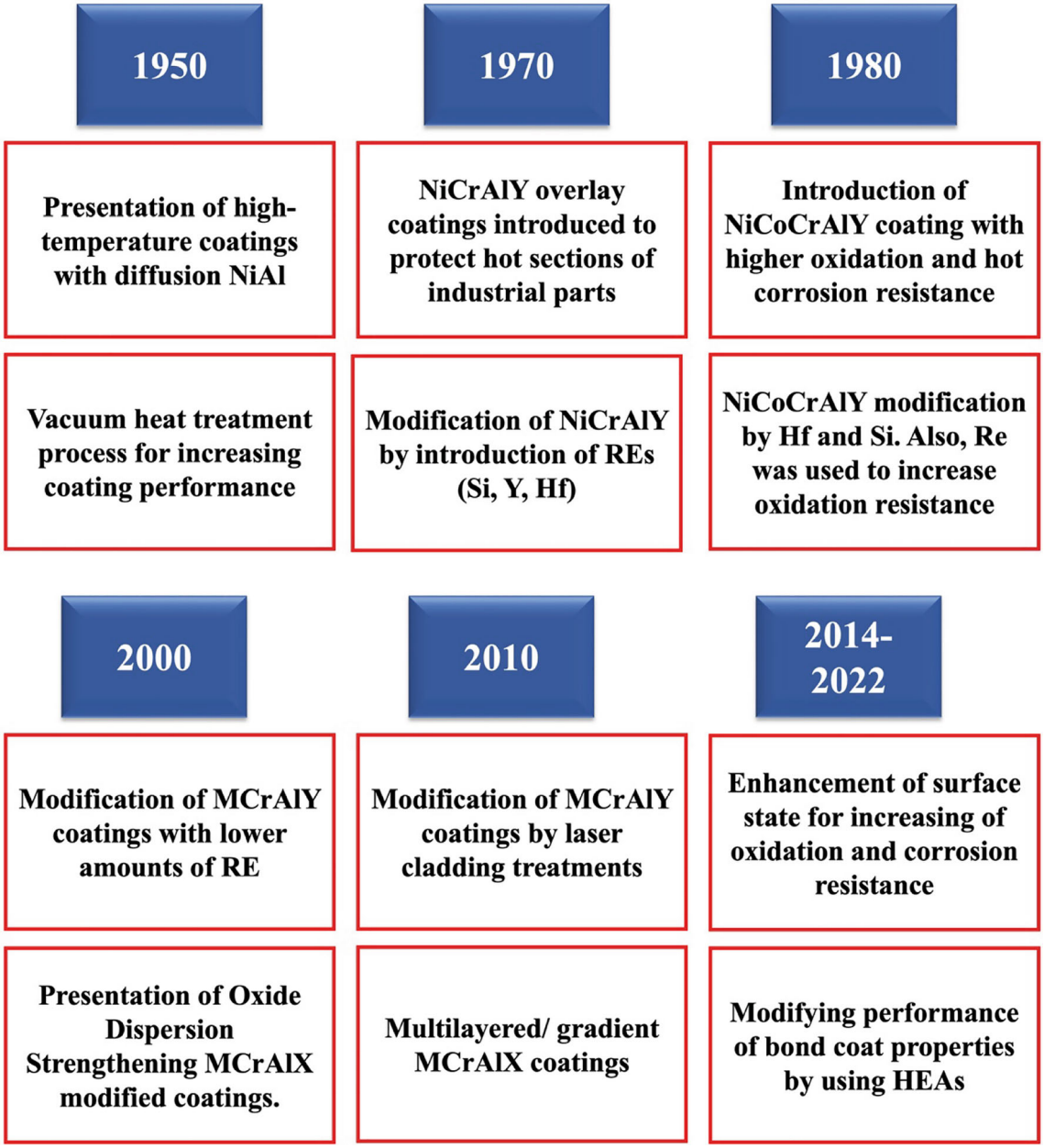

Fig 1 Evolution and Enhancements of MCrAlX Coatings from 1950 to 2022

in various gas turbines (Ref 21). It should be noted that most of the coatings discussed above contain an overall Al content of between 10 and 14 wt.%. Therefore, these coatings were classified as Al_2O_3 formers. Notably, in 1984, the initial iteration of NiCoCrAlY coatings emerged, offering enhanced ductility attributed to the inclusion of cobalt (Co). Moreover, the phase structure of a bond coat plays a significant role in determining its microstructure and composition. MCrAlX coatings typically consist of two primary phases: γ and β. The γ-phase represents a solid solution rich in (Ni, Co) with a face-centerd cubic (FCC) structure, while the β-phase is an intermetallic NiAl (or CoAl) phase characterized by a body-centerd cubic (BCC) structure. Depending on the specific composition, additional phases such as Cr-rich α and Ni_3Al γ' may also be present. The γ-phase has the ability to dissolve various metallic elements, including Fe, Cr, Al, as well as certain refractory metals like Mo, Nb, and Re (22). By acting as an aluminum reservoir, the β-phase enables the formation of a protective Al_2O_3 scale that effectively shields the coating against high-temperature oxidation. The proportion of the β-phase within the coating structure significantly influences its stability and resistance to oxidation at elevated temperatures (Ref 23). Co has been identified as a key element

for enhancing hot corrosion resistance by controlling the fraction of γ'/γ eutectic phases (γ-Ni and γ'-Ni_3Al) within the coating structure (Ref 24). Increasing the cobalt content from 24 to 30 at.% reduces the fraction of γ'-Ni_3Al while increasing the amounts of γ-Ni and β-NiAl, which is attributed to the expansion of the $\gamma + \beta$ region to lower temperatures. The presence of the γ phase (Ni) in the eutectic mixture with γ'-Ni_3Al improves the thermodynamic stability of the coating system. The specific microstructure exhibited by the eutectic phases provides resistance to corrosion attacks (Ref 25). At elevated temperatures, the presence of Co within the Ni-Co-Cr-Al system modifies the phase equilibrium, thereby impeding undesirable phase transitions within the MCrAlX (where X represents reactive elements such as Y, Hf, Ta, Re, Zr, etc.) coating structure (Ref 26). Moreover, the incorporation of Co in the coating structure can augment the solubility of Cr within the γ-phase and eliminate the formation of α-Cr in the microstructure. Consequently, the introduction of Co in NiCoCrAlY coatings has been demonstrated to bolster their mechanical stability (Ref 24). In the years following 2000, because of its performance at high temperatures, modifications of MCrAlX were performed, specifically through work on reactive elements. Due to the increase in TBC lifetime requirement at elevated temperatures, these have been studied extensively (Ref 23, 27). A recent study of MCrAlX coatings has looked at the effects of doping, multilayered/graded design, and surface conditions on the thermal properties of the coatings (Ref 23). After the discovery of HEAs in 2004 by Yeh (Ref 28) and its application to coatings in 2014, potential performance improvement was expected for BCs operating at higher temperatures (Ref 29).

HEA Composition Selection for Bond Coats

Selecting suitable HEA feedstocks for thermal spray applications is challenging. The microstructure and properties of the resulting coatings depend on the process, synthesis routes, and HEA composition. Interestingly, identical alloy compositions can yield coatings with diverse characteristics by adjusting feedstock synthesis techniques and thermal spray parameters. This flexibility enables the customization of coatings for specific applications, including oxidation resistance, corrosion resistance, wear resistance, and enhanced plasticity. To explore different compositions and predict their phase composition and properties, high-throughput experiments and computational techniques are valuable tools (Ref 30). The range of thermal spray processes provides opportunities to manipulate HEA coating characteristics and tailor them to meet specific application requirements (Ref 31). HEAs, with their unique and promising properties, exhibit the potential to serve as viable alternatives to commercial MCrAlX materials. When searching for ways to enhance HEA compositions, several key properties of bond coats should be taken into account: (a) High oxidation resistance: The formation of a protective TGO primarily comprising α-Al_2O_3, the most favorable oxide scale, is essential. During the initial oxidation stage, non-protective oxides such as Cr_2O_3 and NiO are formed due to the sluggish diffusion of Al from the bond coat to the surface. Although Al exhibits higher reactivity toward oxygen compared to Cr and Ni, its diffusion rate is insufficient to sustain the exclusive formation of the α-Al_2O_3 scale (Ref 32). TGO spinel types (AB_2O_4), such as spinel Ni (Cr, Al $)_2O_4$, are considered less desirable due to their brittleness and lower adhesion compared to α-Al_2O_3. The presence of such spinel phases may have an impact on the microstructure of the HEA bond coat (Ref 33). The presence of titanium and silicon in HEAs promotes the formation of Al_2O_3, contributing to improved oxidation resistance. However, it should be noted that the addition of Ti and Si may lead to reduced mechanical properties and the occurrence of rumpling phenomena within the HEAs (Ref 34). (b) Compatibility, Ductility, Integrity: HEAs used in bond coat applications require compatibility with nickel-based alloys as substrates. This is achieved by incorporating Ni or other alloying elements, including Co, Cr, Cu, Fe, Mn, Pd, and Pt, which maintain a stable solid solution structure at high temperatures without undergoing phase transitions with nickel. In addition to compatibility, HEA compositions must exhibit ductility to achieve the desired strength-ductility trade-off necessary for bond coat applications. This allows for accommodating higher fracture toughness. Incorporating multiple phases, such as FCC and BCC structures, effectively fulfills this requirement. To preserve the structural integrity of TBC systems during thermal cycling, it is essential to establish a gradual CTE transition between the top coat, bond coat, and substrate. This gradual transition minimizes the risk of separation or detachment of the top coat from the substrate, ensuring the overall structural integrity of the TBC system (Ref 35, 36) (c) High thermal stability: it is crucial that no first-order phase transformations take place within the specified temperature range of application (Ref 36). In conclusion, developing a HEA for a bond coat application requires a careful selection of desirable candidates with specific characteristics. These candidates should demonstrate high oxidation resistance. This can be achieved by prioritizing forming a protective α-Al_2O_3 scale and minimizing the presence of less desirable TGO spinel phases. Compatibility with nickel-based alloys is another crucial aspect, requiring alloying elements that maintain a stable solid solution structure and contribute to ductility, enabling a desired balance between strength and ductility. Moreover,

establishing a gradual CTE transition within the TBC system is vital to ensure structural integrity during thermal cycling. Finally, it is essential to prioritize high thermal stability by avoiding first-order phase transformations within the designated temperature range. By considering these factors, researchers can effectively identify and develop HEA candidates suitable for bond coat applications.

Presently, endeavors have been undertaken to optimize the phase and composition of this alloy category, specifically targeting TBC bond coats, utilizing artificial intelligence and software tools such as PANDAT, FactSage, MTDATA, MatCalc, JMatPro, and Thermo-Calc (Ref 11). However, the modeling of multi-element systems comprising more than four elements is currently constrained by the scarcity of initial data sources, which heavily rely on experimental data (Ref 3). In the realm of thermal spraying, it is envisaged that the amalgamation of prior alloying expertise with artificial intelligence holds the potential to yield improved outcomes. The realm of HEAs presents notable complexities due to the intricate interplay of multiple elements and diverse processing methods. The thermal spray process, characterized by high temperatures and rapid solidification, further complicates the understanding of HEA behavior.

Microstructural Characteristics of Thermally Sprayed HEA Bond Coats

A coating displaying a fine-grained structure generally demonstrates a strong balance between strength and ductility. Consequently, as-sprayed HEA coatings may manifest distinct phase compositions in contrast to their as-cast counterparts (Ref 37, 38). The phase constituents in HEAs are influenced by both the synthesis techniques of the feedstock and the thermal spraying processes. Through mechanical alloying, powders can undergo nanoscale mixing, resulting in improved solid solubility and the formation of solid solution phases prior to thermal processing (Ref 39). Powders subjected to air plasma spray (APS) or HVOF processes experience additional phase transformations as a result of melting or partial melting. In contrast, materials processed through cold spraying retain their composition due to lower processing temperatures. In the case of the Al-Co-Cr-Fe-Ni system, the mechanical alloying process predominantly yields a BCC phase, as the aluminum acts as a stabilizer for the BCC structure during the alloying process (Ref 40).

The microstructure of HEA bond coats can be affected by several factors, such as the presence of oxides and pores, the HEA powder structure (BCC, FCC and/or (BCC + FCC)), the coating parameters (spray distance, substrate roughness, and coating thickness), as well as particle characteristics (dimension and morphology) (Ref 41, 42). Recent research has indicated that the sluggish diffusion, which is a fundamental characteristic of HEAs, can lead to the formation of nanocrystalline structures and hinder the growth of oxide scales at elevated temperatures (Ref 43). This results in an increase in the bond coat oxidation resistance at high temperatures, which will ultimately result in an increase in the TBC lifetime. In most thermally sprayed HEA bond coats, solid solution strengthening mechanisms also contribute to enhancing hardness (Ref 44). In HEAs, the strengthening mechanism primarily involves solid solution strengthening, which arises from significant lattice distortion caused by disparities in atomic sizes among various constituent elements (Ref 45).

The presence of oxides during the spraying process significantly influences the microstructure of HEA bond coat, thereby impacting the spallation of the bond coat layer. Oxidation is a prominent defect observed in thermally sprayed HEA coatings (Ref 46). The rigid nature of randomly distributed oxides, in contrast to the relatively soft HEA matrix, disrupts the chemical uniformity of the coating.

Therefore, the role of oxides becomes crucial, especially in bond coat applications within TBC systems (Ref 47, 48). It is important to note that oxides exhibiting high porosity can compromise corrosion resistance and lead to accelerated failure of components (Ref 49-51). The formation of oxide precipitates is a prominent concern when HEAs consist of elements that are susceptible to oxidation (Ref 52). In contrast, coatings deposited by cold spraying (Ref 15, 17, 36), HVAF (Ref 16), and HVOF (Ref 14, 46) showed minimal oxidation. As an illustration, in the context of CS, the operation temperature is relatively lower (typically at least 500 °C) than the metals' melting point, leading to a diminished amount of particle oxidation. To conclude, through the meticulous selection of thermal spray techniques, elements, and powder feed rate, it is possible to effectively reduce oxide pore formation, thereby mitigating corrosion and minimizing the possibility of component failure.

In a recent study by Ossiansson et al. (Ref 16), two HEA compositions (CrFeCoNi and AlCrFeCoNi) were used and compared to conventional bond coat types (AMDRY-386 and AMPERIT-410.860). The study examined the microstructure of the HVAF-sprayed coating, which displayed a densely packed structure with minimal oxide inclusions. Comparisons were made between the CrFeCoNi coatings, specifically the microstructures of short nozzle (4L4C) and long nozzle (5L4C), revealing greater oxidation and thicker oxide stringers in the former (Ref 42, 53). The length of the spraying nozzle influenced the

coating's density and the thickness of oxide stringers, with longer nozzles resulting in denser coatings and thinner oxide stringers. In-flight oxidation (IFO) potentially occurred in both coatings due to factors like material chemistry and particle size distribution. The presence of 20 at.% of Al in the CrFeCoNi coatings did not significantly contribute to the formation of oxide scales. In contrast, the AlCrFeCoNi coatings exhibited a two-phase microstructure, benefiting from the presence of Al, which enhanced their resistance to oxidation (Ref 54). The AF-386 (NiCoCrAlYSiHf) microstructure demonstrated an even distribution of distinct phases, indicating minimal alteration of the feedstock material during the HVAF-spray process. The APS-coating exhibited lamellar splats with occasional unmolten particles, likely attributed to incomplete melting. APS-410 (NiCoCrAlY) displayed a more porous microstructure characterized by larger interlamellar splat regions, oxide stringers, and globular pores compared to the other coatings (Ref 55).

In the study conducted by Hsu et al. (Ref 46), the researchers investigated the microstructure and chemical composition of thermal-sprayed coatings produced from HEAC1 ($NiCo_{0.6}Fe_{0.2}Cr_{1.5}SiAlTi_{0.2}$) and HEAC2 ($NiCo_{0.6}Fe_{0.2}Cr_{1.3}SiAl$) using three different techniques: APS, HVOF, and Warm Spraying (WS), as illustrated in Fig 2. The APS coatings were characterized by a lamellar structure consisting of a substantial phase along with dispersed oxide stringers, which could be attributed to the elevated temperature during the spraying process. On the other hand, the HVOF technique, characterized by a lower spraying temperature and higher particle velocity. In the case of warm-sprayed HEA coatings, the researchers observed minimal oxide content, which can be attributed to the precise control of particle temperature during the process. Significantly, HVAF processed HEA coatings exhibit a denser microstructure with minimal oxide formation, in contrast to HEA coatings produced via HVOF methods (Ref 34, 56). The presence of dense coatings is highly advantageous for bond coat applications as they effectively protect the substrate against oxidative deterioration and preserve its structural integrity by preventing the formation and growth of detrimental oxides in and around any existing pores. This effectively inhibits any subsequent detrimental oxidation and ensures the preservation of the intended material composition within the deposited coatings (Ref 57).

Ma et al. (Ref 36) conducted thermal cycle testing on TBC specimens with an HVOF-deposited HEA bond coat in a controlled laboratory setting. The specimens were exposed to a temperature of 1150 °C (± 10 °C) in air. Each thermal cycle involved a 60-minute hold at 1150 °C, followed by forced air cooling for 15 minutes. Visual inspections were carried out after each cycle, and the weight of the specimens was measured every 10 cycles. After 100 cycles, the researchers performed microstructural analysis on the TBC samples before and after the cyclic oxidation test at 1150 °C. They also examined the top views of the test samples. No signs of spallation or damage to the TBC were observed in the top view. However, the microstructure of the tested TBC indicated a tendency for cracking and separation of the topcoat near the interface with the HEA bond coat. The weight gain chart demonstrated that there was no further increase in weight after the initial transient oxidation stage, which resulted in a gain of approximately 0.2 mg/cm^2 (Ref 36).

Finally, in a study carried out by Löbel et al. (Ref 58), a comprehensive investigation was undertaken to examine the microstructures of the coatings. The AlCrFeCoNi coating, fabricated using the HVOF process, exhibited a well-defined lamellar structure with visible oxide and partially formed pores between the spray particles. The coating exhibited a porosity level of approximately 0.6 ± 0.2%. Although the individual spray particles displayed a dendritic structure, there was no significant variation in material composition. In contrast, the coatings produced via the HVAF process did not display prominent oxide lamellae due to the decreased thermal input during the coating process, leading to the suppression of oxygen absorption. Additionally, the HVAF coatings demonstrated significantly lower porosity compared to the HVOF coatings, measuring approximately 0.3 ± 0.1%. This meticulous examination of the microstructures provides valuable insights into the distinct characteristics and properties of HVOF and HVAF coatings, thereby enhancing our understanding of their potential applications in various industries.

Table 1 provides a concise compilation of the key properties exhibited by thermally sprayed HEAs tailored for use in bond coat applications. HVAF and HVOF have emerged as the predominant methods employed thus far. Their utilization has proven advantageous due to their comparatively lower operating temperatures, enabling the production of denser structures compared to alternative techniques (APS, flame spray etc.). These denser structures are highly desirable for BC applications within TBC systems.

Effect of Heat Treatments on the Microstructure and Properties of HEA Bond Coats

Heat treatments will generally modify the bond coat microstructure. This can improve its mechanical properties, such as toughness and corrosion resistance. Heat treatments can also be used to modify the phase stability of the bond coat, which improves thermal stability and oxidation

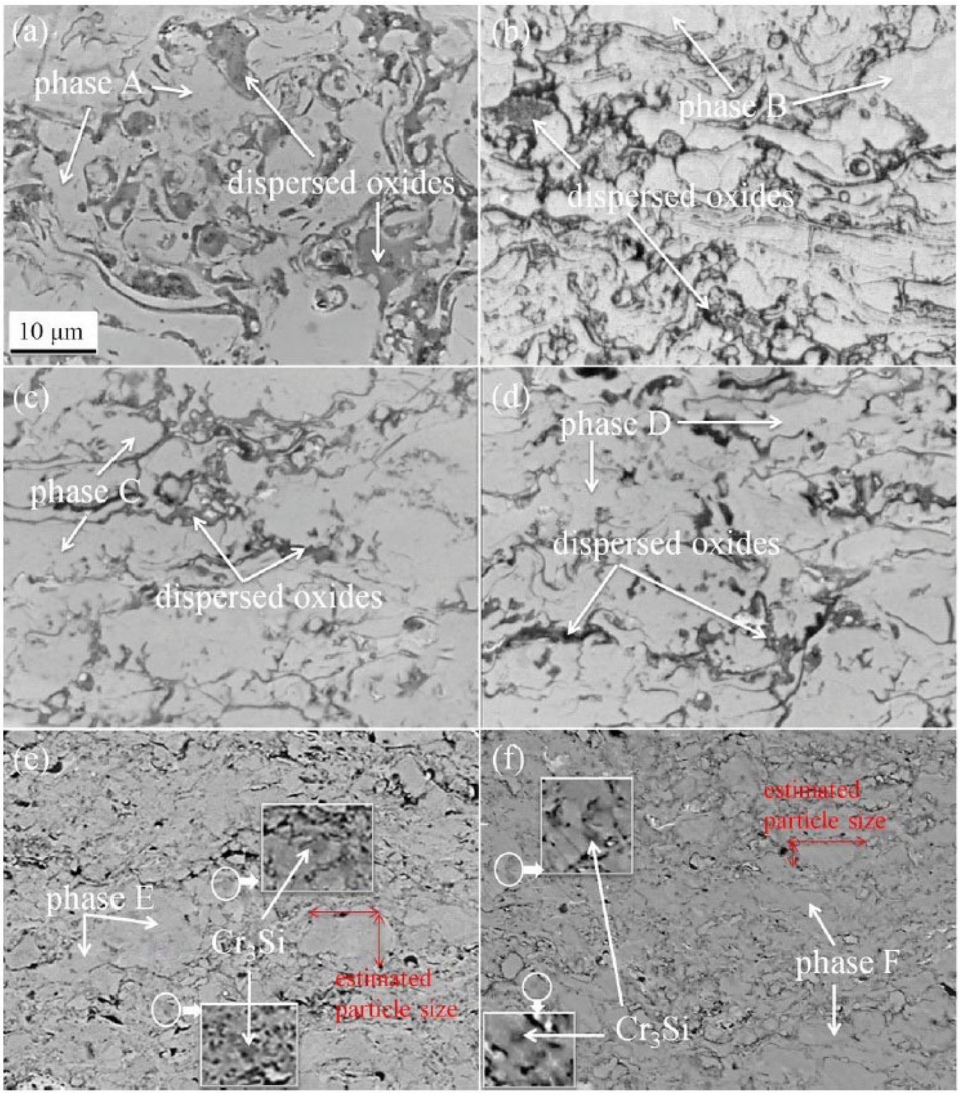

Fig 2 Cross-sectional examinations were performed on the as-sprayed HEA coatings, (a) APS-HEAC1, (b) APS-HEAC2, (c) HVOF-HEAC1, (d) HVOF-HEAC2, (e) WS-HEAC1, and (f) WS-HEAC2 (Ref 46). Used with permission of IOP Publishing, Ltd, from W.-L. Hsu, H. Murakami, H. Araki, M. Watanabe, S. Kuroda, A.-C. Yeh, and J.-W. Yeh, A Study of $NiCo_{0.6}Fe_{0.2}Cr_xSiAlTi_y$ High-Entropy Alloys for Applications as a High-Temperature Protective Coating and a Bond Coat in Thermal Barrier Coating Systems, Journal of the Electrochemical Society, Vol. 165, 2018; permission conveyed through Copyright Clearance Center, Inc.

resistance (Ref 59, 60). Additionally, heat treatments influence the microstructure and phase stability of HEA bond coats and has been extensively investigated (Ref 35). Moreover, heat treatment can be used to tailor the bond coat properties to the specific application and to reduce the risk of bond coat corrosion and oxidation (Ref 60, 61).

Smith et al. (Ref 62) studied a CoCrFeMnNi HEA bond coat, observing that a heat treatment at 1000 °C for 1 hr brought about a fine-grained microstructure. This treatment led to improved mechanical properties, including enhanced strength and ductility, contributing to the bond coat's superior performance. The fine-grained microstructure allowed for better stress distribution throughout the component, increasing strength and ductility. Furthermore, the heat treatment also resulted in a reduction in porosity, which further improved the material's mechanical properties.

In another study by Wu et al. (Ref 63), an AlHfNbTiZr HEA bond coat was examined. A heat treatment at 800 °C induced a transformation from a single-phase solid solution to a dual-phase microstructure. This phase transformation improved the bond coat's thermal stability and resistance to oxidation, making it more capable of withstanding high-temperature environments. Wang et al. (Ref 64) explored a FeCoCrNiCu HEA bond coat using tailored heat treatment processes involving rapid solidification and subsequent annealing. This approach induces the precipitation of coherent nanoscale precipitates within the bond coat's microstructure, enhancing strength and resistance to creep deformation. The study found that the rapid solidification process resulted in a gradient microstructure, with homogeneous, nanometer-sized, coherent precipitates within the matrix. This produced a very strong material with high creep resistance. Furthermore, Chen et al. (Ref 65) investigated an AlCrFeNiTi HEA bond coat. They discovered

Table 1 Properties of HEAs as promising bond coat materials for TBCs

HEA BCs	Coating method	Phases observed	CTE (x 10^{-6}/K)	TGO (thickness μm)	Total hours and max temperature	TGO type	Oxidation behavior
AlCrFeCoNi (Ref 16)	HVAF	BCC	···	At 1000 °C = 3.1 and 4.3	1000 °C 50 h 25 Cycles	Cr_2O_3 & Al_2O_3	No visible spallation was observed (low oxidation rate)
$NiCo_{0.6}Fe_{0.2}Cr_{1.5}SiAlTi_{0.2}$ (Ref 46, 59)	HVOF & WS	FCC + BCC	~13.9	···	1100 °C 336 h 336 Cycles	···	Very good oxidation resistance (at 1100 °C up to 336 cycles)
$AlCoCrNiSi_2$ (Ref 36)	HVOF & APS	B2 + BCC	···	···	1050 °C 200 h 100 Cycles	···	Good oxidation resistance up to 1000 °C
$Ni_{0.2}Co_{0.6}Fe_{0.2}CrSi_{0.2}AlTi_{0.2}$ (Ref 50)	HVOF	BCC	···	···	1100 °C 250 h	···	Specific weight gain = 3.8 mg cm^{-3} (at 1100 °C & 100h)
$Al_{1.4}Co_{2.1}Cr_{0.7}Ni_{2.45}Si_{0.2}Ti_{0.14}$ (Ref 14)	HVOF	FCC + BCC	···	At 1050 °C = 3.7 for 100 cycles	1050 °C 100 h 100 Cycles	Al_2O_3 & $NiAl_2O_4$	Excellent oxidation resistance
MCrAlY (Ref 14)	HVOF	BCC to FCC (With the consumption of NiAl)	···	At 1050 °C = ~ 4 for 100 cycles	1050 °C 100 h 100 Cycles	Al_2O_3 & $NiAl_2O_4$ & Cr_2O_3	Good oxidation resistance up to 1000 °C

FCC: face center cubic

BCC: body center cubic

B2: an order body center cubic

WS: Warm Spray: Modified HVOF technique

MCrAlY: AMDRY 365–4

that a heat treatment at 900 °C for 2 hrs induced secondary phase precipitation, enhancing its corrosion resistance and elevated-temperature stability.

Collectively, these studies demonstrate the significant influence of heat treatment on HEA bond coat microstructure and phase stability. By precisely controlling heat treatment parameters, researchers can manipulate the microstructure, induce favorable phase transformations, and enhance the mechanical properties, thermal stability, oxidation resistance, and creep resistance of HEA bond coats within TBC systems. This means that with careful control of heat treatment, researchers can create bond coats with optimized properties for TBC systems.

Coefficient of Thermal Expansion of HEAs

The extensive utilization of metallic bond coatings in TBCs can be attributed to two key factors. Firstly, it is crucial to consider the disparity in CTE between the YSZ ceramic topcoats ($\sim$10 to 11 $\times$ 10^{-6}/K) and the metallic Ni-based substrates ($\sim$13 $\times$ 10^{-6}/K) (Ref 66, 67). On the contrary, BC materials possess an intermediate CTE, enabling them to serve as an intermediary layer capable of accommodating thermal stresses within the TBC system. Secondly, the presence of bond coats is essential for TBC systems, for which the porous top coat is typically produced through APS, as they provide protection against substrate corrosion and oxidation. In a TBC system, having a high CTE for the topcoat is generally advantageous. The topcoat's high CTE allows it to expand and contract more closely with the underlying substrate and bond coat as they heat and cool during thermal cycling. This close match in CTE helps to reduce the build-up of thermal stresses and strains within the TBC system. By minimizing the thermal mismatch between layers, a high CTE topcoat promotes improved coating adhesion, reduced spallation, and enhanced durability. Therefore, a higher CTE is typically considered beneficial for the topcoat in a TBC system (Ref 68). During cooling, a martensitic phase transformation in substrate superalloys occurs from β to γ phases, which could build up tensile stress in the top coat, which is linearly proportional to E_{TC}*$\Delta\alpha_{TC\text{-}BC}\Delta T$, where E_{TC} is the Young's modulus of the top coat, $\Delta\alpha_{TC\text{-}BC}$ is the difference in thermal expansion between top coat and bond coat, and ΔT is the applied temperature difference (Ref 69).

There is a distinct absence of published studies that specifically investigate the CTE of thermally sprayed HEA bond coats. This prominent research gap underscores a significant void in the current literature, emphasizing the urgent need to address this aspect through further research and comprehensive investigation. Despite the crucial role of the CTE in designing TBC systems, the CTE values of potential HEA bond coats remain unexplored. Limited research exists on the characterization of the CTE of HEAs at elevated temperatures, with only two studies comparing it to MCrAlY materials. These studies highlight the potential of HEAs as alternative materials to conventional MCrAlY, warranting further investigation in the context of TBC systems (Ref 34, 59). The corresponding data can be found in Table 1, and a detailed description of the results is provided in the subsequent paragraph.

Furthermore, it is important to note that the CTEs of the HEA bond coat and YSZ topcoat are closer than the CTEs of MCrAlY bond coat and YSZ. Hsu et al. (Ref 59) conducted a characterization study on a heat-resistant coating composed of a HEA with the composition of $NiCo_{0.6}Fe_{0.2}Cr_{1.5}SiAlTi_{0.2}$, specifically designed for high-temperature applications. The research conducted by the authors involved the fabrication of the HEA through spark plasma sintering. The study revealed that the HEA exhibited remarkable thermal stability, elevated hot hardness, reduced thermal conductivity, and a lower CTE in comparison to the MCrAlY counterparts. The CTE of the HEA was then investigated at various temperatures and compared to that of MCrAlY and Ni-based substrates (CMSX4 and Inconel 718). The results demonstrated that the CTE of the HEA increased from 10 to 15 $\times$ 10^{-6}/K within the temperature range of 200 °C to 800 °C, while the MCrAlY exhibited a relatively higher CTE range of 14 to 19 $\times$ 10^{-6}/K at similar temperatures.

Due to its single-phase FCC structure, the MCrAlY showed a higher CTE ($\sim$16.8 $\times$ 10^{-6}/K) value compared to that of $NiCo_{0.6}Fe_{0.2}Cr_{1.5}$-$SiAlTi_{0.2}$ HEA (BCC structure) ($\sim$13.9 $\times$ 10^{-6}/K). This could be attributed to the lower atomic packing factor of BCC (68%) with relatively higher Young's modulus (E) compared to that of FCC-based materials (where FCC has atomic packing factor of 74%). This can be justified as the CTE tends to be higher for materials with a single FCC structure than those with a single BCC structure. Therefore, it is reasonable to use a HEA as a bond coat (with a BCC structure) since the CTE of a single FCC structure, such as MCrAlY, is generally larger than that of a single BCC structure. As a result, the CTE of the HEA bond coat is closer to that of both the topcoat and substrate (Ref 70).

Another study by Jadhav et al. (Ref 34) investigated $FeCoCrNi_2Al$, $FeCoCrNiAl_{0.3}$, NiCoCrAlSi, and $FeCoNiAlTi_{0.4B}$ HEA compositions by means of spark plasma sintering. The evolution of the CTE of several HEA coatings as a function of temperature (200-1200 °C) is presented in Fig. 3, alongside the evolution of the CTE for the Ni-based superalloy (substrate), the standard MCrAlY bond coat, and a generic Al_2O_3 top coat. As can be observed in Fig. 3, the CTE of the materials tends to increase with increasing temperatures. In general, the CTE

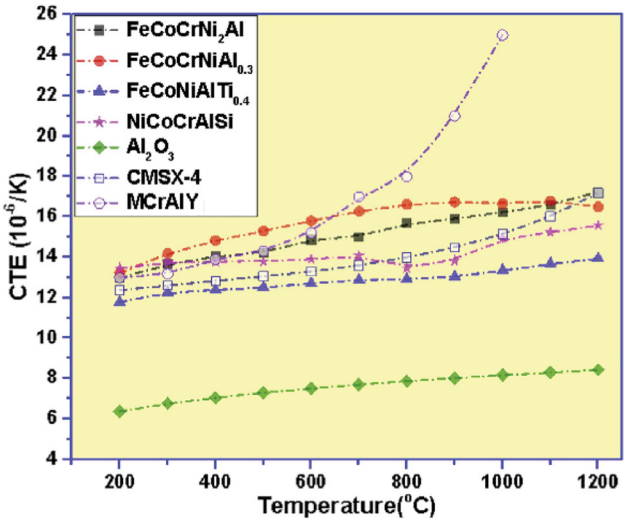

Fig 3 Behavior of the CTE of several HEAs as compared to that of the Ni-based superalloy (CSMX-4), MCrAlY, and Al_2O_3 (Ref 34). Reprinted from Journal of Alloys and Compounds, Vol. 783, Mahesh Jadhav, Sheela Singh, Meenu Srivastava, G.S.Vinod Kumar, An investigation on high entropy alloy for bond coat application in thermal barrier coating system, Pages 662–673, Copyright 2019, with permission from Elsevier

of 6-8 wt.% YSZ is around 10-11. It is desirable for the bond coat CTE to be close to this value. However, there are no studies on the CTE of HEAs used as bond coats. Therefore, using HEAs may offer a promising approach to achieving the desired CTE matching between the bond coat and topcoat (Ref 66, 67, 71). Of notable interest, beyond 800 °C, the CTE of the MCrAlY bond coat visibly increases from the range of 12-16 $\times$ 10^{-6}/K to 25 $\times$ 10^{-6}/K, which shows a certain limitation of this material with increasing temperature. On the other hand, the HEAs retain a CTE that is close to that of the substrate. By tailoring the choice of HEA, such as $FeCoNiAlTi_{0.4}$, it seems possible to choose a HEA that would have an intermediate CTE between the top coat Al_2O_3 and the substrate, further defending the use of HEAs as bond coats.

Oxidation Resistance of HEAs Bond Coat

HEA coatings exhibit favorable resistance to oxidation when compared to conventional materials, indicating promising performance (Ref 72-74). In the context of TBC bond coats, investigations on oxidation behavior are essential, and the manipulation of material design can be influential in regulating oxidation rates. Oxidation resistance is needed when materials are exposed to elevated temperatures in extreme environments (Ref 75). Extensive research efforts have been dedicated to investigating the oxidation behavior of a variety of HEA coatings to gain a comprehensive understanding of their performance in this regard (Ref 31).

Cai et al. (Ref 76) analyzed laser clad $Al_xCrFeCoNi$ HEA coatings, specifically investigating their oxidation behavior. The study revealed that increasing the Al content in the coatings led to reduced oxidation rates. This decrease was attributed to the concurrent formation of $(Al, Cr)_2O_3$ and Al_2O_3. Notably, the presence of an Al_2O_3 TGO layer played a significant role in enhancing the high-temperature oxidation resistance of the coatings. In one study by Huang et al. (Ref 77), $AlSiTiCrFeCoNiMo_{0.5}$ and $AlSiTiCrFeNiMo_{0.5}$ coatings were subjected to oxidation at different temperatures. The coatings demonstrated favorable oxidation resistance up to 1000 °C for 100 hrs due to the formation of protective TiO_2 and Cr_2O_3 layers, which resulted from their slow diffusion.

Bhattacharya et al. (Ref 78) focused on HVOF $Al_{30}Si_2Cr_{23}Co_{22}Ni_{23}$ (at. %) HEA coatings and examined their oxidation at 1050 °C for varying durations. The microstructure of the oxidized coatings consisting of BCC/B2 + FCC + Al_2O_3, with alumina, contributes to their oxidation resistance. The initial weight gain after 100 cycles was significantly lower, measuring 0.2 mg/cm^2, compared to MCrAlX BCs, which typically exhibit a weight gain of 1 mg/cm^2. This lower weight gain can be attributed to the desirable lower thickness and growth rate of the coating. Consequently, HVOF $Al_{30}Si_2Cr_{23}Co_{22}Ni_{23}$ coatings demonstrated excellent oxidation resistance, making them well-suited for aerospace applications.

A recent study by Ossiansson et al. (Ref 16), investigated HEA CrFeCoNi and AlCoCrFeNi coatings sprayed via HVAF for TBC bond coats, to understand the influence of Al in the HEA composition. These coatings were tested in isothermal oxidation, and they were compared to commercially available NiCoCrAlYSiHf and NiCoCrAlY bond coats. These coatings displayed strong adherence of oxide scales without any visible spallation, indicating their effectiveness in resisting oxidation. When compared to conventional MCrAlY coatings, all the tested coatings exhibited a reduced rate of oxidation. The rate of oxidation was evaluated based on the increase in mass per sample area, enabling relative comparisons between the samples rather than absolute values (Ref 79). Figure 4 (Ref 16) illustrates the oxidation behavior of various coatings, including APS-410 (NiCoCrAlY), AF-386 (NiCoCrAlY-SiHf), H2 (HEA: AlCrFeCoNi), and H1 (HEA: CrFeCoNi). APS-410 demonstrated the highest increase in mass per surface area after 1 hr of oxidation, attributed to its lower density and enhanced oxygen diffusion. Conversely, AF-386 exhibited the lowest oxidation rate due to its dense microstructure and distinguished chemistry. H2 coatings, with their higher aluminum content, displayed superior initial oxidation resistance. Surprisingly, H1 coatings,

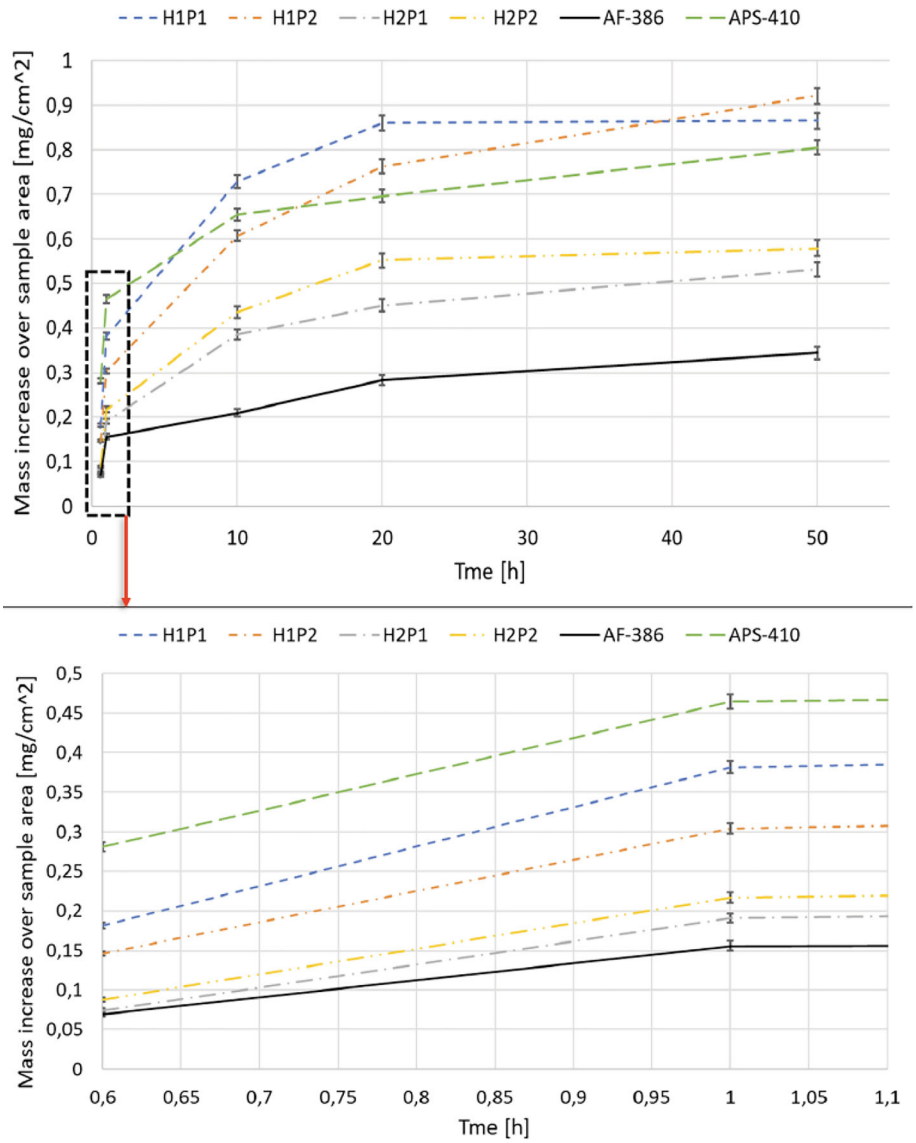

Fig 4 The results obtained from the isothermal oxidation test were depicted graphically, with error bars included to indicate the standard deviation (Ref 16). Reprinted from (Ref 16), available under CC BY 4.0 license at Springer Nature

which had no aluminum content, showed more increase in mass than APS-410 (Ref 55). This suggests the influence of other elements, such as yttrium, in APS-410. Throughout the test, AF-386 consistently maintained a low oxidation rate due to its refined chemistry. After 20 hrs, all samples exhibited a decrease in oxidation rate, attributed to forming a thicker and continuous oxide layer. The study provides valuable insights into the oxidation behavior of coatings. It emphasizes the importance of spraying technique, composition, and material selection in determining performance (Ref 31). The conventional bond coat, as a result, exhibits a lower mass gain, indicating higher oxidation resistance. Furthermore, the HEA with Al content shows a slightly higher mass gain (approximately 0.2 mg/cm^2 after 50 hours) compared to MCrAlY + HfSi. This suggests that the composition of the HEA should be optimized and include reactive elements (Ref 16).

HEAs have the potential to play a direct role in the attainment of a uniform TGO layer, thereby offering enhanced oxidation resistance owing to their participation in the multi-component composition. Accordingly, the controlled consumption of Al and Cr can effectively regulate the formation and growth rates of the TGO layer (Ref 14).

Weight gain in the BCs TBCs system is primarily caused by the formation of oxide scales during oxidation, indicating the degradation of the coating's protective properties, and monitoring weight gain serves as a reliable method for assessing the oxidation behavior and performance of these coatings (Ref 80). In a study by Hsu et al. (Ref 46), thermal-sprayed HEA coatings were subjected to isothermal oxidation tests at 1100 °C. The results, presented in Fig 5, revealed that the HEAC1 ($NiCo_{0.6}Fe_{0.2}Cr_{1.5}SiAlTi_{0.2}$), exhibited rapid weight gain, while the

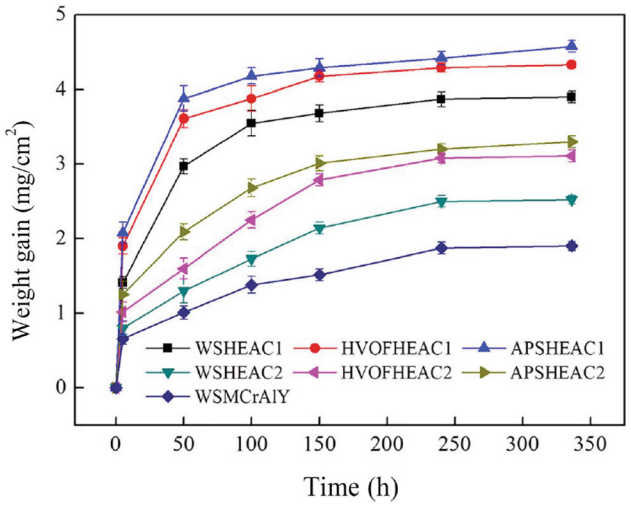

Fig 5 Isothermal oxidation weight gain tests were conducted at 1100 °C to evaluate the weight gain of the thermally sprayed HEAC1 and HEAC2 coatings (Ref 46). Used with permission of IOP Publishing, Ltd, from W.-L. Hsu, H. Murakami, H. Araki, M. Watanabe, S. Kuroda, A.-C. Yeh, and J.-W. Yeh, A Study of $NiCo_{0.6}Fe_{0.2}Cr_xSiAlTi_y$ High-Entropy Alloys for Applications as a High-Temperature Protective Coating and a Bond Coat in Thermal Barrier Coating Systems, Journal of the Electrochemical Society, Vol. 165, 2018; permission conveyed through Copyright Clearance Center, Inc.

HEAC2 ($NiCo_{0.6}Fe_{0.2}Cr_{1.3}SiAl$), showed a slower and more consistent weight gain during initial oxidation (50-100 h). After 250 hrs, all coating specimens displayed minimal additional weight gain. The APS-HEA coatings showed a weight gain increase of 3.1-3.6%, while HVOF and WS-HEA coatings had a weight gain increase of less than 1%. The WS-MCrAlY coating exhibited a weight gain increase of 1.2%. Notably, the HEA coatings demonstrated comparable oxidation resistance to conventional MCrAlY coatings at 1100 °C, indicating their potential as alternative materials for high-temperature applications. Therefore, based on the results of Fig. 5, for the respective HEA bond coats to surpass the oxidation performance of the conventional MCrAlY, a further R&D on the HEA feedstock composition and spray parameter optimization is necessary.

In the recent work, Lu et al. (Ref 72) have performed Y-Hf doping of $AlCoCrFeNi_{2.1}$ by using arc-melting under a Ti-gettered high-purity argon atmosphere, resulting in the formation of a eutectic high-entropy alloy (EHEA). EHEAs, an emerging subgroup within the HEAs category, were introduced with the aim of enhancing liquidity and castability through the incorporation of eutectic principles. To balance high fracture strength and good ductility, eutectic alloys with a mixture of soft FCC and dense BCC phases were proposed. Eutectic alloys, known for their near-equilibrium microstructures, low-energy phase boundaries, and controllable microstructures, have advantageous mechanical properties and castability, making them promising for technological applications in high-temperature alloys. Furthermore, the composite FCC/BCC structure of eutectic HEAs is expected to provide improved mechanical properties and overcome castability obstacles (Ref 81). The alloy has a close symmetrical balance between strength and ductility and is highly resilience against oxidation and spallation under thermal cycling conditions at 1100 °C and 1200 °C after 1008 hrs. Finally, they considered the role of reactive elements doped on the oxidation resistance of bond coat. Remarkably, they discovered that the EHEA illustrated significantly lower oxidation rates at temperatures of 1100 and 1200 °C compared to commercial bond coats such as NiCoCrAlYHf. Additionally, after subjecting the samples to 504 hrs of oxidation at 1200 °C, the scale thickness reached 8.8 ± 0.7 µm for NiCoCrAlYHf, causing severe scale spallation. In contrast, the EHEA exhibited a scale thickness of 10.2 ± 0.5 µm in the same oxidation test, yet the scale remained well-bonded to the alloy (Ref 72).

Another study by Xu et al. (Ref 7) investigated the oxidation characteristics of HEA CuAlNiCrFe compared with a NiCoCrAlY bond coat deposited by a high-speed cladding process. The HEA powders contained a BCC phase, whereas the sprayed coatings contained both FCC and BCC phases. During post-treatment, the bond coat is treated using a diffusion process in a furnace filled with Ar. The low partial pressure of oxygen ensures that only a dense alumina layer is generated (Ref 82). Through the use of high-speed laser cladding, the CuAlNiCrFe high-entropy alloy bond coat can efficiently complete the pre-oxidation and form the α-Al_2O_3 TGO, which shortens the initial oxidation stage and prevents the formation of other oxides and spinel structures. The spinel structures are very brittle and have a lower adherence compared to α-Al_2O_3 and can lead to TBC failure through the combined effects of stress and adherence (Ref 83). Due to the diffusion of aluminum from the bond coat to the top coat, the thickness of the pure alumina-TGO layer increased from 0.89 µm to 3.2 µm, after 4 hrs to 100 hrs of oxidation. The novel CuAlNiCrFe HEA BC compared to the commercial bond coat, demonstrated outstanding oxidation and diffusion resistance by regulating the diffusion between the bonding layer and the substrate (Ref 7).

Jadhav et al. (Ref 34) believed that $FeCoCrNi_2Al$ exhibits excellent oxidation resistance by creating the TGO layer rich in α-Al_2O_3. The TGO layer reaches a thickness of 3 ± 1 µm following 100 hrs of oxidation at 1050 °C. To mitigate the occurrence of localized separations at the interface between the TGO layer and the TBC, the TGO layer must retain its elasticity under high operating temperatures. This elasticity is essential for safeguarding

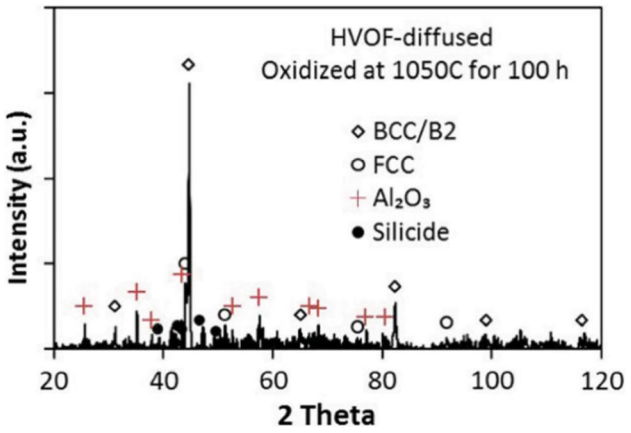

Fig 6 XRD spectrum of an $Al_{30}Co_{22}Cr_{23}Ni_{23}Si_2$ coating following isothermal oxidation at 1050 °C for 100 h. in the air (Ref 36). Reprinted from X. Ma, P. Ruggiero, R. Bhattacharya, O.N. Senkov, Evaluation of New High Entropy Alloy as Thermal Sprayed Bondcoat in Thermal Barrier Coatings, Journal of Thermal Spray Technology, Vol. 31, Pages 1011–1020, Copyright 2021, with permission from Springer Nature

against detrimental effects such as "rumpling" or cavitation that may arise during thermal cycling.

Ma et al. (Ref 36) used an $Al_{30}Co_{22}Cr_{23}Ni_{23}Si_2$ HEA as a bond coat deposited by HVOF to characterize the TGO formation. Figure 6 depicts the XRD pattern obtained from a sample subjected to a 100 hrs. oxidation test at 1050 °C. Following oxidation, the predominant phase observed is the BCC/B2 phase, accompanied by minor peaks representing FCC and Al_2O_3. These findings suggest the thermal stability of the HEA coating, with the oxidation test primarily resulting in the formation of α-Al_2O_3 TGO on the coating's surface. This outcome is favorable for bond coats as it imparts high oxidation resistance at elevated temperatures.

In a recent study conducted by Srivastava et al. (Ref 14), HEA-based and MCrAlY-based TBC coatings with YSZ topcoats were subjected to cyclic oxidation at 1050 °C for 100 cycles. The presence of NiAl-rich phases in the bond coat facilitated the formation of Al_2O_3 at high temperatures. The application of YSZ as a topcoat effectively mitigated accelerated oxidation in both types of coatings. Notably, the HEA coating exhibited reduced waviness in the TGO scale when compared to the MCrAlY coating. The average thickness of the TGO layer, as shown in Table 2 (Ref 14), was found to be similar for both coatings, approximately 3.7 µm and 3.8 µm, respectively, after 100 cycles of oxidation. A study has reported a TGO thickness of approximately 4 mm for a NiCrAlY-based TBC subjected to oxidation at 1050 °C for 100 cycles (Ref 84). These findings contribute valuable insights into the behavior of TBC coatings under cyclic oxidation conditions (Ref 85).

Table 2 The TBC system exhibited variation in the average thickness of the TGO layer as the number of cycles increased (Ref 14)

Cyclic oxidation duration (hrs./Cycle)	Oxide layer thickness (µm)	
	HEA	MCrAlY
25 h	2.1	2.1
50 h	2.2	2.2
100 h	3.7	3.8

Reprinted from Journal of Alloys and Compounds, Vol. 924, Meenu Srivastava, Mahesh S. Jadhav, Chethan, R.P.S. Chakradhar, Sheela Singh, Investigation of HVOF Sprayed Novel $Al_{1.4}Co_{2.1}Cr_{0.7}Ni_{2.45}Si_{0.2}Ti_{0.14}$ HEA Coating as Bond Coat Material in TBC System, Page 166388, Copyright 2022, with permission from Elsevier

Currently, only two studies have specifically examined TGO parameters in HEA bond coats. However, these studies have not observed any noteworthy variations in TGO properties (thickness, uniformity, and slowing of growth rate), when compared to conventional commercial bond coat materials. As shown in Table 1, it is clear that there is a need for greater emphasis on improving the thickness control and uniformity of the TGO layer in HEAs, especially at elevated temperatures. HEA composition and spray parameters can be optimized in order to achieve this goal. Commonly, the thickness of the TGO layer is regarded as an essential factor in determining the remaining lifetime of a TBC system, particularly when thermal cycles and associated thermal stresses are present. As a result, TGO thickness increases, and it could cause top coat failure by producing stresses and cracking. Moreover, according to Table 1, some TGO types (Al_2O_3, Cr_2O_3, $NiAl_2O_4$) are related to a certain portion of the composition elements. In order to achieve the desired TGO layer composed of α-Al_2O_3, the presence of Al is typically required. Collectively, HEA coatings exhibit better oxidation resistance than conventional bond coat materials (MCrAlX). Material design manipulations, such as increasing aluminum content or incorporating reactive elements, can enhance performance. Based on these findings, HEA coatings can be used for high-temperature applications, emphasizing the importance of the coating's oxidation behavior when developing advanced protective coatings.

Future Outline

To advance and optimize the potential of HEAs for bond coat applications, future research and development should prioritize key aspects. This includes addressing cost reduction, improved formability, and gaining a comprehensive understanding of the influence of processing

parameters on HEA bond coat properties. Experimental studies should focus on various areas such as composition design, property optimization, alloy processing and fabrication, phase stability, microstructure control, application-specific investigations, CTE, and environmental considerations. Additionally, simulation studies should explore atomistic and molecular dynamics simulations, phase stability predictions, mechanical properties modeling, high-temperature oxidation and corrosion simulations, interface and adhesion modeling, as well as multiscale and multi-physics simulations. By addressing these aspects, the field of HEAs can advance significantly, leading to wider industrial adoption and commercialization, particularly in bond coat applications (Ref 31, 41, 75).

Furthermore, the exploration of HEAs faces challenges in the future due to their extensive composition and microstructure space, which renders conventional trial-and-error methods inefficient. To overcome this, the implementation of combinatorial studies utilizing high-throughput techniques becomes crucial. These studies play a vital role in identifying undesirable materials and designing high-performance HEAs more effectively (Ref 86). By enabling researchers to focus on understanding the design and manufacture of high-performance HEAs, particularly in the turbine industries, valuable time spent on repetitive sample preparation and characterization can be minimized.

Conclusion

HEAs have gained significant attention as alternatives to conventional materials for surface engineering bond coats in TBC systems. It is expected that their outstanding properties, including high oxidation and corrosion resistance, as well as the ability to form uniform and dense TGO layers, position HEAs as potential substitutes for MCrAlY bond coat materials. Extensive studies on thermal spray coatings have investigated various aspects such as thermal expansion, phase transition temperature, hardness, and oxidation resistance, revealing the outstanding oxidation resistance of HEA thermal spray coatings and their potential to replace conventional bond coat materials. HEA bond coats have the potential to exhibit lower thermal conductivity than MCrAlY BCs, leading to improved cooling efficiency in TBC systems. The enhanced phase stability of HEAs at high temperatures and in oxidizing environments further makes them appealing as promising materials for TBCs. Utilizing HEAs for TBC bond coatings has demonstrated similar behavior to MCrAlY materials at high temperatures (<1000 °C), effectively mitigating corrosion and surface damage while facilitating the formation of a thin, dense, and continuous Al_2O_3 layer on the bond coat surface. Further research is needed to explore HEA compositions and spraying techniques to achieve superior performance compared to MCrAlY at elevated temperatures (>1100 °C) and potentially extend the TBC lifetime. Additionally, investigating factors such as CTE, TGO behavior, and optimizing HEA compositions are crucial to maximize their potential in bond coating applications and enhance performance and durability.

Acknowledgments This work was conducted as part of the project entitled "Engineering the Next Generation of Thermal Barrier Coatings (TBCs) Via Thermal Spraying", supported by the National Research Council of Canada (NRC) Surftec Industrial R&D Group, as well as the NRC's National Program Office. The authors would like to acknowledge the NRC, as well as, the Surftec Industrial R&D Group members that supported this investigation and publication, the Consortium de recherche et d'innovation en transformation métallique (CRITM) for funding through its Support Program for Research and Innovation Organizations (PSO), and NRC's academic collaborator to this project, Concordia University.

References

1. R.S. Lima, Porous APS YSZ TBC. Manufactured at High Powder Feed Rate (100 g/Min) and Deposition Efficiency (70%): Microstructure, Bond Strength and Thermal Gradients, *J. Therm. Spray Technol.*, 2022, **31**, p 396-414.
2. V. Jalilvand, S. Mohammadkhani, F. ben Ettouil, L. Roué, A. Dolatabadi, D. Guay and C. Moreau, The Effect of Bond Coat on the High-Temperature Behavior of HVOF-Sprayed (Co, Ni)O Coating on Cu-Ni-Fe Anodes, *Surf. Coat. Technol.*, 2022, **441**, p 128576.
3. Y. Zhang, T.T. Zuo, Z. Tang, M.C. Gao, K.A. Dahmen, P.K. Liaw and Z.P. Lu, Microstructures and Properties of High-Entropy Alloys, *Prog. Mater. Sci.*, 2014, **61**, p 1-93.
4. D.R. Clarke, M. Oechsner and N.P. Padture, Thermal-Barrier Coatings for More Efficient Gas-Turbine Engines, *MRS Bull.*, 2012, **37**(10), p 891-898.
5. A.C. Karaoglanli, Structure and Durability Evaluation of Blast Furnace Slag Coatings and Thermal Barrier Coatings (TBCs) under High Temperature Conditions, *Surf. Coat. Technol.*, 2023, **452**, p 129087.
6. D. Pan, M.W. Chen, P.K. Wright and K.J. Hemker, Evolution of a Diffusion Aluminide Bond Coat for Thermal Barrier Coatings during Thermal Cycling, *Acta Mater.*, 2003, **51**(8), p 2205-2217.
7. Q.L. Xu, Y. Zhang, S.H. Liu, C.J. Li and C.X. Li, High-Temperature Oxidation Behavior of CuAlNiCrFe High-Entropy Alloy Bond Coats Deposited Using High-Speed Laser Cladding Process, *Surf. Coat. Technol.*, 2020, **398**, p 126093.
8. W.R. Chen, X. Wu, B.R. Marple, D.R. Nagy and P.C. Patnaik, TGO Growth Behaviour in TBCs with APS and HVOF Bond Coats, *Surf. Coat. Technol.*, 2008, **202**(12), p 2677-2683.
9. J. He, Advanced MCrAlY Alloys with Doubled TBC Lifetime, *Surf. Coat. Technol.*, 2022, **448**, p 128931.
10. J. Rahimi, M.R. Javadi-Sigaroodi and E. Poursaeidi, Thermal Shock Resistance of Thermal Barrier Coating with Different Bondcoat Types and Diffusion Pre-Coating, *Ceram. Int.*, 2022, **49**, p 2061-2072.
11. B.S. Murty, *High-Entropy Alloys*, Butterworth-Heinemann, Oxford, 2014.
12. N. Hidayah and B. Nordin, "Phase Transformation in High Entropy Bulk Metallic Glass (HE-BMG) and Lamellar Structured-High Entropy Alloy (HEA)," 2018.

13. M. Garg, H.S. Grewal, R.K. Sharma, B. Gwalani and H.S. Arora, Limiting Oxidation of High Entropy Alloy via High Strain-Rate Deformation: Insights from Electrochemical Impedance Spectroscopy, *Mater. Chem. Phys.*, 2023, **294**, p 127017.
14. M. Srivastava, M.S. Jadhav, R.P.S. Chakradhar and S. Singh, Investigation of HVOF Sprayed Novel $Al_{1.4}Co_{2.1}Cr_{0.7}Ni_{2.45}Si_{0.2}Ti_{0.14}$ HEA Coating as Bond Coat Material in TBC System, *J. Alloys Compd.*, 2022, **924**, p 166388.
15. R. Supekar, R.B. Nair, A. McDonald and P. Stoyanov, Sliding Wear Behavior of High Entropy Alloy Coatings Deposited through Cold Spraying and Flame Spraying: A Comparative Assessment, *Wear*, 2023, **516-517**, p 204596.
16. M. Ossiansson, M. Gupta, M. Löbel, T. Lindner, T. Lampke and S. Joshi, Assessment of CrFeCoNi and AlCrFeCoNi High-Entropy Alloys as Bond Coats for Thermal Barrier Coatings, *J. Therm. Spray Technol.*, 2022, **31**(4), p 1404-1422.
17. C.J. Akisin, C.J. Bennett, F. Venturi, H. Assadi and T. Hussain, Numerical and Experimental Analysis of the Deformation Behavior of CoCrFeNiMn High Entropy Alloy Particles onto Various Substrates During Cold Spraying, *J. Therm. Spray Technol.*, 2022, **31**, p 1085-1111.
18. P. Zhang, R.L. Peng, X.-H. Li, S. Johansson, P. Xiao, Linköpings universitet. Institutionen för ekonomisk och industriell utveckling, and Linköpings universitet. Tekniska fakulteten, "Performance of MCrAlX Coatings Oxidation, Hot Corrosion and Interdiffusion," LiU-Tryck, 2019, p 4-61.
19. M.R. Jackson and J.R. Rairden, Diffusion Paths in the Ni-Cr-Al Ternary Diagram for Formation and Degradation of Oxidation-Resistant Coating, *Thin Solid Films*, 1977, **45**(3), p 376.
20. R. Lowrie and D.H. Boone, Composite Coatings of CoCrA1Y Plus Platinum, *Thin Solid Films*, 1977, **45**, p 491-498.
21. D. Fayeulle and M. Jeandin, Thermal Barrier Coatings with Cellular Electrophoretic Bond Coats, *J. Manuf. Process.*, 1990, **5**(3), p 419-426.
22. V. der, genehmigte Dissertation, H.H. Dr-Ing habil Oettel, T.H. Bergakademie Freiberg Herr Dr-Ing habil Biermann, and T.R. Bergakademie Freiberg Herr Dr-Ing Bürgel, "The Influence of Cobalt and Rhenium on the Behaviour of MCrAlY Coatings," 2004.
23. F. Ghadami, A. Sabour Rouh Aghdam and S. Ghadami, Microstructural Characteristics and Oxidation Behavior of the Modified MCrAlX Coatings: A Critical Review, *Vacuum*, 2021, **185**, p 109980.
24. K. Schneider and H.W. Grunling, 416 metallurgical and protective coatings 395 mechanical aspects of high temperature coatings, *Thin Solid Films*, 1983, **107**, p 395-416.
25. J.J. Liang, H. Wei, Y.L. Zhu, X.F. Sun, T. Jin, Z.Q. Hu, M.S. Dargusch and X. Yao, Influence of Co Addition on Constituent Phases and Performance of a NiCrAlYRe Alloy System, *Surf. Coat. Technol.*, 2011, **205**(21-22), p 4968-4979.
26. D.R.G. Achar, R. Munoz-Arroyo, L. Singheiser and W.J. Quadakkers, Modelling of Phase Equilibria in MCrAlY Coating Systems, *Surf. Coat. Technol.*, 2004, **187**(2-3), p 272-283.
27. Q. Liu, S. Huang and A. He, Composite Ceramics Thermal Barrier Coatings of Yttria Stabilized Zirconia for Aero-Engines, *JMST*, 2019, **35**, p 2814-2823.
28. M.C. Gao, J.-W. Yeh, P.K. Liaw and Y. Zhang, *High-Entropy Alloys*, Springer, Berlin, 2016.
29. X.W. Qiu, Y.P. Zhang and C.G. Liu, Effect of Ti Content on Structure and Properties of $Al_2CrFeNiCoCuTi_x$ High-Entropy Alloy Coatings, *J. Alloys Compd.*, 2014, **585**, p 282-286.
30. C.C. Berndt, "Introduction to Materials Production for Thermal Spray Processes," 2004.
31. A. Meghwal, A. Anupam, B.S. Murty, C.C. Berndt, R.S. Kottada and A.S.M. Ang, Thermal Spray High-Entropy Alloy Coatings: A Review, *J. Therm. Spray Technol.*, 2020, **29**, p 857-893.
32. R.J. Takahashi, J.M.K. Assis, F. Piorino-Neto and D.A.P. Reis, Heat Treatment for TGO Growth on NiCrAlY for TBC Application, *Mater Res Express*, 2019, **6**(12), p 126442.
33. V. Teixeira, M. Andritschky, W. Fischer, H.P. Buchkremer and D. Stöver, Effects of Deposition Temperature and Thermal Cycling on Residual Stress State in Zirconia-Based Thermal Barrier Coatings, *Surf. Coat. Technol.*, 1999, **120**, p 103-111.
34. M. Jadhav, S. Singh, M. Srivastava and G.S. Vinod Kumar, An Investigation on High Entropy Alloy for Bond Coat Application in Thermal Barrier Coating System, *J. Alloys Compd.*, 2019, **783**, p 662-673.
35. J. Yu, R. Mu, S. Qu, Y. Cai and Z. Shen, The Effect of Heat Treatment at 1200 °C on Microstructure and Mechanical Properties Evolution of AlCoCrFeNiSiYHf High Entropy Alloys, *Vacuum*, 2022, **200**, p 111039.
36. X. Ma, P. Ruggiero, R. Bhattacharya, O.N. Senkov, and A.K. Rai, Evaluation of New High Entropy Alloy as Thermal Sprayed Bondcoat in Thermal Barrier Coatings, *J. Therm. Spray Technol.*, 2022, 1011-1020.
37. P.K. Huang, J.W. Yeh, T.T. Shun and S.K. Chen, Multi-Principal-Element Alloys with Improved Oxidation and Wear Resistance for Thermal Spray Coating, *Adv. Eng. Mater.*, 2004, **6**(1-2), p 74-78.
38. C.C. Tung, J.W. Yeh, T. tsung Shun, S.K. Chen, Y.S. Huang and H.C. Chen, On the Elemental Effect of AlCoCrCuFeNi High-Entropy Alloy System, *Mater. Lett.*, 2007, **61**(1), p 1-5.
39. M. Vaidya, G.M. Muralikrishna and B.S. Murty, High-Entropy Alloys by Mechanical Alloying: A Review, *J. Mater. Res.*, 2019, **34**, p 664-686.
40. A. Anupam, S. Kumar, N.M. Chavan, B.S. Murty and R.S. Kottada, First Report on Cold-Sprayed AlCoCrFeNi High-Entropy Alloy and Its Isothermal Oxidation, *J. Mater. Res.*, 2019, **34**(5), p 796-806.
41. P. Patel, A. Roy, N. Sharifi, P. Stoyanov, R. Chromik and C. Moreau, Tribological Performance of High-Entropy Coatings (HECs): A Review, *Materials*, 2022, **15**(10), p 3699.
42. K. Torkashvand, M. Gupta, S. Björklund, F. Marra, L. Baiamonte and S. Joshi, Influence of Nozzle Configuration and Particle Size on Characteristics and Sliding Wear Behaviour of HVAF-Sprayed WC-CoCr Coatings, *Surf. Coat. Technol.*, 2021, **423**, p 127585.
43. M. Arshad, M. Amer, Q. Hayat, V. Janik, X. Zhang, M. Moradi and M. Bai, High-Entropy Coatings (HEC) for High-Temperature Applications: Materials, Processing, and Properties, *Coatings*, 2022, **12**, p 691.
44. R.B. Nair, G. Perumal and A. McDonald, Effect of Microstructure on Wear and Corrosion Performance of Thermally Sprayed AlCoCrFeMo High-Entropy Alloy Coatings, *Adv. Eng. Mater.*, 2022, **24**(9), p 2101713.
45. M.H. Tsai and J.W. Yeh, High-Entropy Alloys: A Critical Review, *Mater Res Lett*, 2014, **2**(3), p 107-123.
46. W.-L. Hsu, H. Murakami, H. Araki, M. Watanabe, S. Kuroda, A.-C. Yeh and J.-W. Yeh, A Study of $NiCo_{0.6}Fe_{0.2}CrxSiAlTiy$ High-Entropy Alloys for Applications as a High-Temperature Protective Coating and a Bond Coat in Thermal Barrier Coating Systems, *J. Electrochem. Soc.*, 2018, **165**(9), p C524-C531.
47. G. Mauer, R. Vaen and D. Stöver, Plasma and Particle Temperature Measurements in Thermal Spray: Approaches and Applications, *J. Therm. Spray Technol.*, 2011, **20**, p 391-406.
48. M.P. Planche, H. Liao and C. Coddet, Oxidation Control in Atmospheric Plasma Spraying Coating, *Surf. Coat. Technol.*, 2007, **202**(1), p 69-76.
49. Q. Wei, Z. Yin and H. Li, Oxidation Control in Plasma Spraying NiCrCoAlY Coating, *Appl. Surf. Sci.*, 2012, **258**(12), p 5094-5099.
50. W.L. Hsu, H. Murakami, J.W. Yeh, A.C. Yeh and K. Shimoda, On the Study of Thermal-Sprayed $Ni_{0.2}Co_{0.6}Fe_{0.2}CrSi_{0.2}AlTi_{0.2}$ HEA Overlay Coating, *Surf. Coat. Technol.*, 2017, **316**, p 71-74.

51. R.A. Neiser, M.F. Smith and R.C. Dykhuizen, Oxidation in Wire HVOF-Sprayed Steel, *J. Therm. Spray Technol.*, 1998, **7**, p 537-545.
52. A. Anupam, R.S. Kottada, S. Kashyap, A. Meghwal, B.S. Murty, C.C. Berndt and A.S.M. Ang, Understanding the Microstructural Evolution of High Entropy Alloy Coatings Manufactured by Atmospheric Plasma Spray Processing, *Appl. Surf. Sci.*, 2020, **505**, p 144117.
53. V. Matikainen, H. Koivuluoto, P. Vuoristo, J. Schubert and S. Houdková, Effect of Nozzle Geometry on the Microstructure and Properties of HVAF-Sprayed WC-10Co_4Cr and Cr_3C_{2-25}NiCr Coatings, *J. Therm. Spray Technol.*, 2018, **27**(4), p 680-694.
54. W. Brandl, H.J. Grabke, D. Toma and J. Kruger, The Oxidation Behaviour of Sprayed MCrAlY Coatings, *Surf. Coat. Technol.*, 1996, **86**, p 41-47.
55. P. Niranatlumpong, C.B. Ponton and H.E. Evans, The Failure of Protective Oxides on Plasma-Sprayed NiCrAlY Overlay Coatings, *Oxid. Met.*, 2000, **53**(3), p 241-258.
56. A.S.M. Ang, C.C. Berndt, M.L. Sesso, A. Anupam, R.S. Kottada and B.S. Murty, Plasma-Sprayed High Entropy Alloys: Microstructure and Properties of AlCoCrFeNi and MnCoCrFeNi, *Metall. Mater. Trans. A Phys. Metall. Mater. Sci.*, 2015, **46**(2), p 791-800.
57. M. Löbel, T. Lindner and T. Lampke, High-Temperature Wear Behaviour of AlCoCrFeNi$Ti_{0.5}$ Coatings Produced by HVOF, *Surf. Coat. Technol.*, 2020, **403**, p 126379.
58. M. Löbel, T. Lindner, T. Mehner, L.M. Rymer, S. Björklund, S. Joshi and T. Lampke, Microstructure and Corrosion Properties of AlCrFeCoNi High-Entropy Alloy Coatings Prepared by HVAF and HVOF, *J. Therm. Spray Technol.*, 2022, **341**, p 247-255.
59. W.-L. Hsu, H. Murakami, J.-W. Yeh, A.-C. Yeh and K. Shimoda, A Heat-Resistant $NiCo_{0.6}$ $Fe_{0.2}$ $Cr_{1.5}SiAlTi_{0.2}$ Overlay Coating for High-Temperature Applications, *J Electrochem Soc, The Electrochemical Society*, 2016, **163**(13), p C752-C758.
60. M.R.J. Sigaroodi, E. Poursaeidi, J. Rahimi and Y.Y. Jamalabad, Heat Treatment Effect on Coating Shock Resistance of Thermal Barrier Coating System with Different Types of Bond Coat, *J. Eur. Ceram. Soc.*, 2023, **43**(8), p 3658-3675.
61. J. Rahimi, M.R. Javadi Sigaroodi and E. Poursaeidi, Thermal Shock Resistance of Thermal Barrier Coating with Different Bondcoat Types and Diffusion Pre-Coating, *Ceram. Int.*, 2023, **49**(2), p 2061-2072.
62. T.J. Smith, Synthesis and Mechanical Properties of Direct Laser Sintered High Entropy Alloys, 2020.
63. Y. Wu, J. Si, D. Lin, T. Wang, W.Y. Wang, Y. Wang, Z.K. Liu and X. Hui, Phase Stability and Mechanical Properties of AlHfNbTiZr High-Entropy Alloys, *Mater. Sci. Eng. A*, 2018, **724**, p 249-259.
64. H. Wang, Z. Wu, H. Wu, H. Zhu and W. Tang, In Situ TiC Particle-Reinforced FeCoCrNiCu High Entropy Alloy Matrix Composites by Induction Smelting, *Trans. Indian Inst. Met.*, 2021, **74**(2), p 267-272.
65. L. Chen, K. Bobzin, Z. Zhou, L. Zhao, M. Öte, T. Königstein, Z. Tan and D. He, Wear Behavior of HVOF-Sprayed $Al_{0.6}$-TiCrFeCoNi High Entropy Alloy Coatings at Different Temperatures, *Surf Coat Technol*, 2019, **358**, p 215-222.
66. J. Yuan, J. Sun, J. Wang, H. Zhang, S. Dong, J. Jiang, L. Deng, X. Zhou and X. Cao, $SrCeO_3$ as a Novel Thermal Barrier Coating Candidate for High-Temperature Applications, *J Alloys Compd*, 2018, **740**, p 519-528.
67. W. Ma, D.E. MacK, R. Vaßen and D. Stöver, Perovskite-Type Strontium Zirconate as a New Material for Thermal Barrier Coatings, *J. Am. Ceram. Soc.*, 2008, **91**(8), p 2630-2635.
68. T. Hayase, H. Waki and K. Adachi, Residual Stress Change in Thermal Barrier Coating Due to Thermal Exposure Evaluated by Curvature Method, *J. Therm. Spray Technol.*, 2020, **29**(6), p 1300-1312.
69. R. Vaßen, G. Kerkhoff and D. Stö, Development of a Micromechanical Life Prediction Model for Plasma Sprayed Thermal Barrier Coatings, *Mater. Sci. Eng.*, 2001, **300**, p 100-109.
70. H.P. Chou, Y.S. Chang, S.K. Chen and J.W. Yeh, Microstructure, Thermophysical and Electrical Properties in AlxCoCrFeNi ($0 \leq x \leq 2$) High-Entropy Alloys, *Mater. Sci. Eng. B Solid State Mater. Adv. Technol.*, 2009, **163**(3), p 184-189.
71. M.A. Helminiak, N.M. Yanar, F.S. Pettit, T.A. Taylor and G.H. Meier, The Behavior of High-Purity, Low-Density Air Plasma Sprayed Thermal Barrier Coatings, *Surf. Coat. Technol.*, 2009, **204**(6-7), p 793-796.
72. J. Lu, H. Zhang, L. Li, Y. Chen, X. Liu, X. Zhao and F. Guo, Y-Hf Co-Doped AlCoCrFeNi$_{2.1}$ Eutectic High-Entropy Alloy with Excellent Oxidation and Spallation Resistance under Thermal Cycling Conditions at 1100 °C and 1200 °C, *Corros Sci*, 2021, **187**, p 109515.
73. J. Lu, Y. Chen, H. Zhang, L. He, R. Mu, Z. Shen, X. Zhao and F. Guo, Y/Hf-Doped $Al_{0.7}$CoCrFeNi High-Entropy Alloy with Ultra Oxidation and Spallation Resistance at 1200°C, *Corros Sci*, 2020, **174**, p 108803.
74. J. Lu, H. Zhang, L. Li, A. Huang, X. Liu, Y. Chen, X. Zhang, F. Guo and X. Zhao, Y-Hf Co-Doped $Al_{1.1}CoCr_{0.8}$FeNi High-Entropy Alloy with Excellent Oxidation Resistance and Nanostructure Stability at 1200°C, *Scr. Mater.*, 2021, **203**, p 114105.
75. R. Bhaskaran Nair, R. Supekar, S. Morteza Javid, W. Wang, Y. Zou, A. McDonald, J. Mostaghimi and P. Stoyanov, High-Entropy Alloy Coatings Deposited by Thermal Spraying: A Review of Strengthening Mechanisms Performance Assessments and Perspectives on Future Applications, *Metals*, 2023, **13**(3), p 579.
76. Y. Cai, L. Zhu, Y. Cui, K. Geng, S. Marwana-Manladan and Z. Luo, High-Temperature Oxidation Behavior of FeCoCrNiAlx High-Entropy Alloy Coatings, *Mater Res Express*, 2019, **6**(12), p 126552.
77. P.K. Huang, J.W. Yeh, T.T. Shun and S.K. Chen, Multi-Principal-Element Alloys with Improved Oxidation and Wear Resistance for Thermal Spray Coating, *Adv Eng Mater*, 2004, **6**(1-2), p 74-78.
78. R. Bhattacharya, O.N. Senkov, A.K. Rai, X. Ma, and P. Ruggiero, "High Entropy Alloy Coatings for Application as Bond Coating for Thermal Barrier Coating Systems," A. Agarwal, G. Bolelli, A. Concustell, Y.-C. Lau, A. McDonald, F.-L. Toma, E. Turunen, and C.A. Widener, Eds., 2016, p 279-285.
79. H. Choi, B. Yoon, H. Kim and C. Lee, Isothermal Oxidation of Air Plasma Spray NiCrAlY Bond Coatings, *Surf. Coat. Technol.*, 2002, **150**, p 297-308.
80. D. Zhang, S. Gong, H. Xu and Z. Wu, Effect of Bond Coat Surface Roughness on the Thermal Cyclic Behavior of Thermal Barrier Coatings, *Surf. Coat. Technol.*, 2006, **201**(3), p 649-653.
81. Y. Lu, Y. Dong, S. Guo, L. Jiang, H. Kang, T. Wang, B. Wen, Z. Wang, J. Jie, Z. Cao, H. Ruan and T. Li, A Promising New Class of High-Temperature Alloys: Eutectic High-Entropy Alloys, *Sci Rep*, 2014, **4**, p 6200.
82. M. Karadge, X. Zhao, M. Preuss and P. Xiao, Microtexture of the Thermally Grown Alumina in Commercial Thermal Barrier Coatings, *Scr. Mater.*, 2006, **54**(4), p 639-644.
83. D.M. Nissley, Thermal Barrier Coating Life Modeling in Aircraft Gas Turbine Engines, *J. Therm. Spray Technol.*, 1997, **3**(6), p 91-989.

84. L. Shi, L. Xin, X. Wang, X. Wang, H. Wei, S. Zhu and F. Wang, Influences of MCrAlY Coatings on Oxidation Resistance of Single Crystal Superalloy DD98M and Their Inter-Diffusion Behaviors, *J. Alloys Compd.*, 2015, **649**, p 515-530.
85. Y. Zhang, X. Liang, D. Zhang, M. Tan and E.P. Xing, Unsupervised Object-Level Video Summarization with Online Motion Auto-Encoder, *Pattern Recognit. Lett.*, 2020, **130**, p 376-385.
86. S. Mooraj and W. Chen, A Review on High-Throughput Development of High-Entropy Alloys by Combinatorial Methods, *JMI*, 2023, **3**(1), p 4.